

# Optical measurement and modeling of interactions between two hole or two electron spins in coupled InAs quantum dots

A. Greilich<sup>1,2</sup>, Ș. C. Bădescu<sup>1,3</sup>, D. Kim<sup>1,4</sup>, A. S. Bracker<sup>1</sup>, D. Gammon<sup>1</sup>

<sup>1</sup>Naval Research Laboratory, Washington, DC 20375, USA

<sup>2</sup>Technische Universität Dortmund, 44221 Dortmund, Germany

<sup>3</sup>Air Force Research Laboratory, Wright-Patterson AFB, OH 45433, USA

<sup>4</sup>Harvard University, Cambridge, MA 02138, USA

(Dated: November 14, 2018)

Two electron spins in quantum dots coupled through coherent tunneling are generally acknowledged to approximately obey Heisenberg isotropic exchange. This has not been established for two holes. Here we measure the spectra of two holes and of two electrons in two vertically stacked self-assembled InAs quantum dots using optical spectroscopy as a function of electric and magnetic fields. We find that the exchange is approximately isotropic for both systems, but that significant asymmetric contributions, arising from spin-orbit and Zeeman interactions combined with spatial asymmetries, are required to explain large anticrossings and fine-structure energy splittings in the spectra. Asymmetric contributions to the isotropic Hamiltonian for electrons are of the order of a few percent while those for holes are an order of magnitude larger.

PACS numbers: 71.70.Ej, 71.70.Gm, 78.55.Cr, 78.67.Hc

The exchange interaction between the spins in two quantum dots (QDs) leads to entanglement and to the opportunity of quantum information processing [1]. Electron spin qubits have been studied in great detail, but recently hole spins have received special attention [2, 3] because of their reduced hyperfine interaction with the nuclear spin reservoir [4–7]. Now, for inter-QD entanglement, the nature of the exchange interaction is of central importance, both for quantum gates and for decoherence of two-qubit states [8–10].

The symmetry of the exchange interaction is often assumed to be the Heisenberg isotropic exchange,  $J\sigma_1 \cdot \sigma_2$ . As a result, the eigenstates of two spins in two quantum dots form singlet and triplet spin states separated by the exchange energy,  $J$ . This model is very important, conceptually [1] and for interpretations of complex experimental spectra [11–13], and has been used widely in magnetism, quantum computing, molecular and quantum dot structures. It has been shown that for two bound electrons the isotropic Heisenberg interaction captures almost all of the physics and it requires only small asymmetric exchange terms that couple singlets and triplets [14–19].

In contrast to electron spins, hole spins are in some ways extremely anisotropic; for example, in their  $g$ -factor [20] and in their hyperfine interaction [21]. This anisotropy arises from the strong spin-orbit character of the valence band, and is complicated by heavy-light hole mixing. Counterintuitively, we find through optical spectroscopy that isotropic exchange between two self-assembled InAs QDs is in fact a good starting point for both two electrons and for two holes [22] [23]. Nevertheless substantial asymmetric contributions arising from spin-orbit interactions are necessary to explain anticrossings in the optical spectra. In addition, inhomoge-

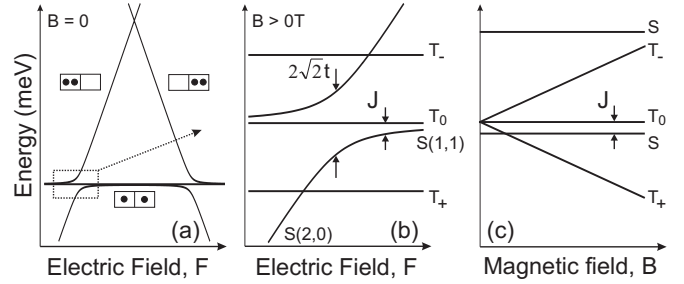


FIG. 1. (a) Hund-Mulliken model for two-spin configuration at zero  $B$ . (b)  $F$  dependence at fixed  $B$  for a symmetric case, Eq. (2). (c)  $B$  dependence at fixed  $F$  (marked by arrows with  $J$  in (b)).

neous Zeeman interactions, that is, differences in the  $g$ -factor between the two QDs and also in the tunnel barrier, lead to additional energy splittings in the optical spectra that grow with magnetic field. All of these interactions lead to off-diagonal spin mixing terms that can be accounted for in a generalized spin Hamiltonian.

In this paper we use individual pairs of vertically stacked self-assembled InAs/GaAs QDs separated by a thin tunnel barrier with a thickness  $d$ . Two types of samples were developed using a Schottky diode grown by molecular beam epitaxy, one for  $2h$  [3] and one for  $2e$  [12]. To obtain a direct comparison, the width and height of the tunnel barriers were chosen to achieve similar values of singlet-triplet splitting for both cases ( $J \approx 100 \mu\text{eV}$ ) [24]. Electric ( $F$ ) and magnetic ( $B$ ) fields were applied longitudinally along the stacking  $z$ -axis in the Faraday geometry. The optical spectra were measured at 5 K using photoluminescence with a spectral resolution limited by the triple spectrometer of  $\sim 15 \mu\text{eV}$  for the  $2h$  case, and laser transmission spectroscopy with a

resolution of  $< 1 \mu\text{eV}$  for the  $2e$  case.

The Heisenberg exchange can be treated within the Hund-Mulliken model [25, 26]. The natural spin state basis is three triplets:  $T_0 = (\uparrow, \downarrow)_{T_0}$ ,  $T_+ = (\uparrow, \uparrow)_{T_+}$ ,  $T_- = (\downarrow, \downarrow)_{T_-}$  and three singlets:  $S_{(2,0)} = (\uparrow\downarrow, 0)_S$ ,  $S_{(1,1)} = (\uparrow, \downarrow)_S$ , and  $S_{(0,2)} = (0, \uparrow\downarrow)_S$ . The individual spin projections are either the electron spin  $\pm 1/2$  or hole pseudo-spin  $\pm 1/2$ . The singlet states are coupled together and shifted in energy by spin conserving tunneling ( $t$ ) between the two QDs, but because of spin blocking, the triplet states are not affected. The Hamiltonian within the singlet basis is given by:

$$\begin{pmatrix} (\uparrow\downarrow, 0)_S & (\uparrow, \downarrow)_S & (0, \uparrow\downarrow)_S \\ Fd + U & -\sqrt{2}t & 0 \\ -\sqrt{2}t & 0 & -\sqrt{2}t \\ 0 & -\sqrt{2}t & -Fd + U \end{pmatrix} \quad (1)$$

The potential ( $U$ ) is the Coulomb energy required to move the two charges from separate QDs to the same QD. The relative energy between QDs separated by  $d$  is controlled via  $F$ . In Fig. 1(a), the resulting levels of the singlets show anticrossings. The lowest energy singlet state is  $S = aS_{(2,0)} + bS_{(1,1)} + cS_{(0,2)}$ . In Fig. 1(b) and hereafter we focus on one of the anticrossings, and take  $c = 0$ . The isotropic exchange interaction  $J$  is defined as the splitting between  $T_0$  and the lowest singlet with the spin Hamiltonian  $J\sigma_1 \cdot \sigma_2$ , with  $J = J(F, U, t)$ .

To fully probe and engineer the spin states of the two QDs we also need, in addition to  $F$ , a magnetic field  $B$ . The simplest Hamiltonian consists of isotropic exchange and an average Zeeman interaction,

$$J\sigma_1 \cdot \sigma_2 + \beta^{ext} \cdot (\sigma_1 + \sigma_2) \quad (2)$$

The Zeeman term  $\beta^{ext} = (g_{11} + g_{22})\mu_B \mathbf{B}/2$  splits the  $T_+$  and  $T_-$  lines, but preserves the spin states.  $\mu_B$  is the Bohr magneton. (1 and 2 mark the bottom and top dot, respectively.) In Fig. 1(b) the energies are calculated as a function of  $F$  with  $B$  held constant, while in Fig. 1(c) the reverse is done.

The optical spectrum arises from transitions between the  $2e$  levels and the charged exciton levels ( $X^{2-}$ ) as shown in Fig. 2(a). Here we show the calculated dependence on  $B$ , holding  $F$  constant. The exciton states have been described previously [11, 26]. The optical spectrum is found by taking the difference between the  $2e$  and ( $X^{2-}$ ) levels and weighting according to the selection rules. The results for the  $2e$ 's, which are fits to the measured spectra, are shown in Fig. 2(b). As measured in previous studies, a singlet line at  $B = 0$  splits into two with increasing  $B$ . Likewise, the triplet line also splits into two, although each of these lines is doubly degenerate. However, at high  $B$  these lines also split, although the splitting is very small for this  $2e$  case and requires the high resolution of laser spectroscopy to resolve. The

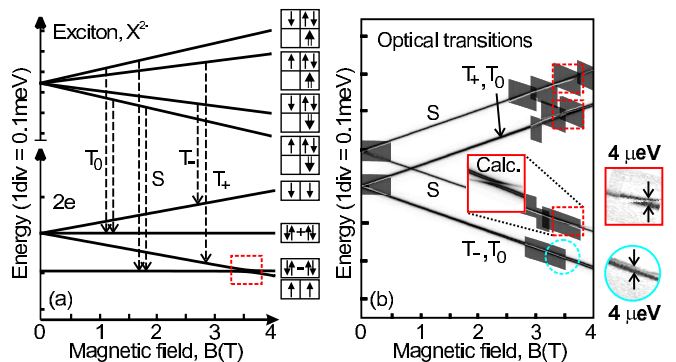


FIG. 2. (color online) (a) Calculated  $B$  dependence for the excited and ground states obtained by fitting the  $2e$  transmission spectra. Transitions are labeled by final state. (b) Fitted optical spectrum for the  $2e$  case using the parameters:  $g_{e,11} = g_{e,22} = -0.49$ ,  $g_{h,22} = 1.58$ ,  $t = 350 \mu\text{eV}$ ,  $U = 10 \text{ meV}$ . Diamagnetic shift of  $8.9 \mu\text{eV}/\text{T}^2$  is subtracted. Shaded areas are the laser transmission measurements with the boxes to the right representing an expanded views of the data at  $B = 3.5 \text{ T}$ .

lowest inset on the right side of the figure shows the measured splitting at  $B = 3.5 \text{ T}$  with a value of  $4 \mu\text{eV}$ . The splitting grows to  $8 \mu\text{eV}$  at  $B = 5.6 \text{ T}$ . We will show below that this fine-structure splitting of the triplet arises from asymmetric Zeeman terms. In addition there are small anticrossings that occur only at  $B = 3.5 \text{ T}$  as shown in the square insets on the right side of Fig. 2(b). These anticrossings occur where the  $2e$  singlet and triplet energy levels would cross as seen in Fig. 2(a), and arise from asymmetric exchange due to spin-orbit interactions. Other than these spin-flip anticrossings and the triplet fine-structure splitting that grows with  $B$ , the symmetric approximation is very good for the  $2e$  spectrum.

In contrast to the  $2e$  case of Fig. 2(b), the measured  $2h$  spectrum appears much more complex as shown in Fig. 3(a). In addition to substantial fine-structure splittings observed in the triplet optical transitions that grow with increasing  $B$  ( $36 \mu\text{eV}$  at  $3.5 \text{ T}$ ), there are now obvious anticrossings with magnitudes of  $26 \mu\text{eV}$  at  $B = 1.5 \text{ T}$  that can be observed even in photoluminescence, though with the resolution of a triple spectrometer. We have also measured the  $2h$  optical spectrum as a function of  $F$  at fixed  $B$ . The complex pattern of anticrossings observed in the data of Fig. 3(d) arises from the spin-flip anticrossings in combination with the larger spin-conserving anticrossings of both the  $2h$  and the exciton states that have been described previously [26, 27]. Remarkably, with the same formalism for both the  $2e$  and the  $2h$  cases, all of these features can be explained with natural extensions of the symmetric Hamiltonian, Eq. (2). As a result we obtain the fitted optical transition spectrum shown in Figs. 3(b) and 3(e), and calculate the corresponding  $2h$  energy levels in Figs. 3(c) and 3(f). A comparison of these  $2h$  energy levels and those of the symmetric calculations of Fig. 1 show clearly the importance of asymmetric spin

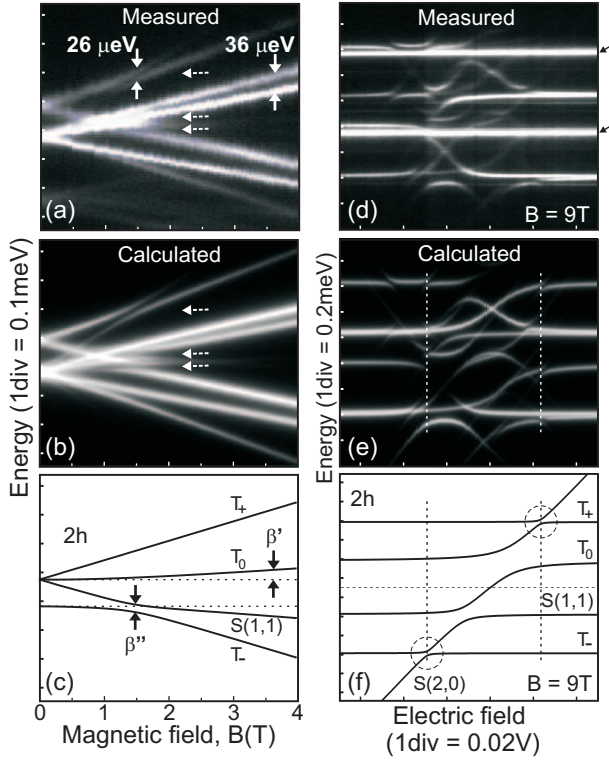


FIG. 3. (a) measured and (b) calculated transition spectra of  $B$  dependence for the  $X^{2+}$ .  $g_{h,11} = 1.85$ ,  $g_{h,22} = 0.78$ ,  $g_{e,22} = -0.46$ ,  $g_{h,12} = 0.14$ ,  $t = -115 \mu\text{eV}$ ,  $\gamma_{12} = 24 \mu\text{eV}$ ,  $\Delta\gamma \sim 5 \mu\text{eV}$ . In calculation  $S = \sqrt{0.44}S_{(2,0)} + \sqrt{0.56}S_{(1,1)}$ . (a) and (b) Three signatures of anticrossings are marked by dashed horizontal arrows. Diamagnetic shift of  $11.6 \mu\text{eV}/\text{T}^2$  is subtracted in (a). (c) Calculated  $2h$  energy levels with ground state  $S/T_-$  anticrossing of  $26 \mu\text{eV}$ . (d) measured and (e) calculated transition spectra of  $F$  dependence for  $B = 9 \text{ T}$ . (small black arrows on the right of panel (d) mark a transition spectra of  $X^+$ .) (f) Ground state energy levels as a function of bias. Circles mark the spin-flip anticrossings. Vertical lines mark the position of anticrossings in transition spectra of Fig. 3(d) and 3(e).

interactions.

We generalize the symmetric spin Hamiltonian of Eq. (2) to include spin coupling terms as follows. The spin interaction of holes (or electrons) again is included with interaction terms,  $\beta_1^{tot} \cdot \sigma_1 + \beta_2^{tot} \cdot \sigma_2$  acting on each spin. The fields now include not only the external magnetic field but also the internal relativistic magnetic field arising from the spin-orbit interaction  $\beta_i^{tot} = \beta_i^{ext} + \beta_i^{so}$ . We could also include the Overhauser field due to the hyperfine interaction with nuclear spins, in a similar way to Ref. [19], but this is expected to be small here. After integrating over the orbital degrees of freedom and including the isotropic exchange we obtain the general spin Hamiltonian for two spins in two QDs:

$$J\sigma_1 \cdot \sigma_2 + \beta \cdot (\sigma_1 + \sigma_2) + \beta' \cdot (\sigma_1 - \sigma_2) + \beta'' \cdot (\sigma_1 \times \sigma_2) \quad (3)$$

In our case, the strong axis of the QDs and also the

external  $B$  are along the  $z$ -axis,  $\mathbf{B} = B\hat{z}$ . The QDs are also stacked along the  $z$ -axis. We take the lateral asymmetry (e.g., an offset  $d$  between the centers of the QDs) to have  $\beta^{so} = \gamma\hat{x}$ . This displacement generates a gauge factor  $e^{i\phi_B}$  between the QDs,  $\phi_B \propto Bd$  [28]. In Eq. (3),  $\beta' = \text{Re}\langle S|\beta^{tot}|T\rangle$  and  $\beta'' = \text{Im}\langle S|\beta^{tot}|T\rangle$  can be written in terms of the Zeeman and spin-orbit fields ( $\alpha = \mu_B B/2$ ):

$$\beta = \alpha\Sigma g\hat{z} + \Sigma\gamma\hat{x} \quad (4)$$

$$\beta' = \alpha(ag_{12}^{Re} + b\Delta g)\hat{z} + (a\gamma_{12}^{Re} + b\Delta\gamma)\hat{x} \quad (5)$$

$$\beta'' = \alpha ag_{12}^{Im}\hat{z} + a\gamma_{12}^{Im}\hat{x}. \quad (6)$$

The Zeeman interaction with the external  $B$  is determined by the matrix elements of the coordinate-dependent  $g$ -factor  $g(r)$  over the two QDs:  $\Sigma g = (g_{11} + g_{22})$ ,  $\Delta g = (g_{11} - g_{22})$  and  $g_{12} = \langle 1|g(r)|2\rangle e^{i\phi_B}$ . Likewise, the spin-orbit field leads to mixing terms given by matrix elements of  $\gamma$ . The linear superposition  $aS_{(2,0)} + bS_{(1,1)}$  gives a contribution of  $\Delta\gamma$  and  $\gamma_{12}$ , which is determined by measuring its dependence on  $F$ . The experiment gives absolute values  $|g_{12}|$  and  $|\gamma_{12}|$ .

We can also write the Hamiltonian of Eq. (3) in a matrix form within the singlet/triplet spin basis that shows explicitly how the states are mixed, and permits convenient fitting to the data.

$$\begin{pmatrix} (\uparrow\downarrow, 0)_S & (\uparrow, \downarrow)_S & (\uparrow, \downarrow)_{T_0} & (\uparrow, \uparrow)_{T_+} & (\downarrow, \downarrow)_{T_-} \\ Fd + U & -\sqrt{2}t & \alpha\sqrt{2}g_{12} & \gamma_{12} & -\gamma_{12} \\ -\sqrt{2}t & 0 & \alpha\Delta g & -\Delta\gamma & \Delta\gamma \\ \alpha\sqrt{2}g_{12}^* & \alpha\Delta g & 0 & \Sigma\gamma & \Sigma\gamma \\ \gamma_{12}^* & -\Delta\gamma & \Sigma\gamma & \alpha\Sigma g & 0 \\ -\gamma_{12}^* & \Delta\gamma & \Sigma\gamma & 0 & -\alpha\Sigma g \end{pmatrix} \quad (7)$$

Here we explicitly include both singlet states and the tunneling rate  $t$  (instead of  $J$ ) for convenience in fitting the data.

The off-diagonal terms lead to the observed anticrossings and fine-structure splittings in the spectra. The phenomenological Zeeman and spin-orbit parameters,  $g_{ij}$  and  $\gamma_{ij}$ , have useful physical interpretations, and can each be associated with specific features in the spectra. First, the term with  $\Delta g$  is manifesting the difference in  $g$ -factors between the two QDs, and likely arises from the difference in size and indium concentration between the two QDs. This parameter is larger for holes than for electrons in part because the larger effective mass of the hole makes them more localized and more sensitive to differences of the QDs such as differences in size or composition. The term with  $g_{12}$  physically arises from the difference in  $g$ -factor between the barrier and the QDs, which leads to the  $\uparrow$  and  $\downarrow$  spins-tunneling at different rates [29, 30]. These terms breaks the spin symmetry and mixes  $S$  and  $T_0$ , effectively pushing the  $S$  and  $T_0$  energies apart as a function of  $B$  as seen in Fig. 3(c). This is measured directly in the optical spectrum by the fine-structure splitting in the triplet transitions that grows

with  $B$ . The splitting is given by  $\beta'$  in Eq. (5). At sufficiently high fields the eigenstates become  $(\uparrow, \downarrow)$  and  $(\downarrow, \uparrow)$ , instead of  $(\uparrow, \downarrow)_S$  and  $(\uparrow, \downarrow)_{T_0}$  [31].

The result of the spin-orbit field is similar but with an important difference. The spin-orbit field acting orthogonal to  $\hat{z}$  has the effect of partially rotating  $\uparrow$  to  $\downarrow$ , and vice versa. In particular, the term  $\gamma_{12}$ , which couples  $(\uparrow\downarrow, 0)_S \leftrightarrow (\uparrow, \uparrow)_{T_-}$ , can be viewed as spin-flip tunneling. It is analogous to the spin conserving tunneling term ( $t$ ), which couples  $(\uparrow\downarrow, 0)_S \leftrightarrow (\uparrow, \downarrow)_S$  [32]. The  $\gamma_{12}$  term along with the  $\Delta\gamma$  term have the effect of mixing the  $S$  state with the  $T_-$  and  $T_+$  triplet states, and leads to the anticrossing observed in Fig. 3(c) with magnitude given by  $\beta''$  in Eq. (6).

The term  $\Sigma\gamma$  couples  $T_0$  with the  $T_+$  and  $T_-$  triplets. It can be measured as a splitting of the triplet line at zero  $B$ . Any zero-field splitting of the triplet energies was found to be less than our resolution, and so we took this parameter to be zero [33]. We note that in a separate study there is evidence for a finite splitting of  $\sim 8 \mu\text{eV}$  for the  $2h$  case in a similar sample from coherent measurements in the time domain [3]. Additionally, Ref. [27] represents a short description of a microscopic origin of these spin mixing terms.

Using Eq. (7) we are able to get good fits to the data with the coupling parameters given in Table I.

TABLE I. Electron and hole coupling parameters:

	$\Sigma g$	$\Delta g$	$ g_{12} $	$\Sigma\gamma(\mu\text{eV})$	$\Delta\gamma(\mu\text{eV})$	$ \gamma_{12} (\mu\text{eV})$
hole	2.63	1.07	0.14	0	5	24
electron	0.98	0	0.3	0	2	3

In conclusion, we have found that a symmetric spin Hamiltonian based on the isotropic Heisenberg exchange interaction can be generalized to treat the  $2h$  as well as the  $2e$  spectrum in tunnel-coupled QDs using phenomenological off-diagonal Zeeman and spin-orbit parameters. The fact that the  $2h$  exchange interaction between QDs is primarily Heisenberg-like is important, because it means that concepts and techniques developed for the control of  $2e$  spins can potentially be used for  $2h$ 's. Moreover, the substantial spin mixing that can occur at the anticrossing points and at large magnetic fields is also potentially useful for spin control and/or measurement. Such mixings have already been used to propose and demonstrate simultaneous optical spin-flip and cycling transitions for a single electron spin [34]. As another example, quantum control of two holes could also be obtained with electrostatic gates (instead of optical gates) in a way analogous to Taylor *et al.* [35]. However, instead of hyperfine coupling, the much larger spin-orbit interaction could be used, thereby enabling faster gates.

- 
- [1] D. Loss and D. P. DiVincenzo, Phys. Rev. A **57**, 120 (1998).
  - [2] K. De Greve, P. L. McMahon, D. Press, T. D. Ladd, D. Bisping, C. Schneider, M. Kamp, L. Worschech, S. Höfling, A. Forchel, and Y. Yamamoto, Nat. Phys. **7**, 872 (2011).
  - [3] A. Greilich, S. G. Carter, D. Kim, A. S. Bracker, and D. Gammon, Nat. Photon. **5**, 702 (2011).
  - [4] D. Brunner, B. D. Gerardot, P. A. Dalgarno, G. Wst, K. Karrai, N. G. Stoltz, P. M. Petroff, and R. J. Warburton, Science **325**, 70 (2009).
  - [5] B. Eble, C. Testelin, P. Desfonds, F. Bernardot, A. Balocchi, T. Amand, A. Miard, A. Lemaître, X. Marie, and M. Chamarro, Phys. Rev. Lett. **102**, 146601 (2009).
  - [6] P. Fallahi, S. T. Yılmaz, and A. Imamoglu, Phys. Rev. Lett. **105**, 257402 (2010).
  - [7] E. A. Chekhovich, A. B. Krysa, M. S. Skolnick, and A. I. Tartakovskii, Phys. Rev. Lett. **106**, 027402 (2011).
  - [8] G. Burkard, D. Loss, and D. P. DiVincenzo, Phys. Rev. B **59**, 2070 (1999).
  - [9] G. Burkard, G. Seelig, and D. Loss, Phys. Rev. B **62**, 2581 (2000).
  - [10] R. I. Dzhioev, K. V. Kavokin, V. L. Korenev, M. V. Lazarev, B. Y. Meltser, M. N. Stepanova, B. P. Zakharchenya, D. Gammon, and D. S. Katzer, Phys. Rev. B **66**, 245204 (2002).
  - [11] M. Scheibner, M. F. Doty, I. V. Ponomarev, A. S. Bracker, E. A. Stinaff, V. L. Korenev, T. L. Reinecke, and D. Gammon, Phys. Rev. B **75**, 245318 (2007).
  - [12] D. Kim, S. G. Carter, A. Greilich, A. S. Bracker, and D. Gammon, Nat. Phys. **7**, 223 (2011).
  - [13] K. M. Weiss, J. M. Elzerman, Y. L. Delle, J. Miguel-Sanchez, and A. Imamoglu, Phys. Rev. Lett. **109**, 107401 (2012).
  - [14] K. V. Kavokin, Phys. Rev. B **64**, 075305 (2001).
  - [15] S. C. Bădescu, Y. B. Lyanda-Geller, and T. L. Reinecke, Phys. Rev. B **72**, 161304 (2005).
  - [16] S. Chutia, M. Friesen, and R. Joynt, Phys. Rev. B **73**, 241304 (2006).
  - [17] F. Baruffa, P. Stano, and J. Fabian, Phys. Rev. Lett. **104**, 126401 (2010).
  - [18] M. P. Nowak and B. Szafran, Phys. Rev. B **82**, 165316 (2010).
  - [19] D. Stepanenko, M. Rudner, B. I. Halperin, and D. Loss, Phys. Rev. B **85**, 075416 (2012).
  - [20] T. Andlauer and P. Vogl, Phys. Rev. B **79**, 045307 (2009).
  - [21] J. Fischer and D. Loss, Phys. Rev. Lett. **105**, 266603 (2010).
  - [22] K. V. Kavokin, Phys. Rev. B **69**, 075302 (2004).
  - [23] As a counter example, electron-hole exchange in the case of the neutral exciton is nearly Ising-like ( $J\sigma_{ez}\sigma_{hz}$ ) with two nearly degenerate doublets separated by the exchange splitting. In that case, a small asymmetric  $e$ - $h$  exchange  $\delta(\sigma_x^h\sigma_y^e + \sigma_y^h\sigma_x^e)$  mixes the two bright excitons. Another example is the case of two holes in a single QD – one in the s-shell and the other in the p-shell. In contrast to two electrons in a single QD, the energy structure deviates strongly from isotropic, and is apparently neither Heisenberg-like nor Ising-like [36].
  - [24] For the hole sample we have used a Be-doped GaAs

- buffer, 25 nm GaAs spacer, 2.8 nm InAs bottom dot, 6 nm GaAs tunnel barrier, 3.2 nm InAs top dot, followed by 280 nm GaAs capping layer. The electron sample was similar but with a 9 nm barrier composed of 3/3/3 nm of GaAs/Ga<sub>0.7</sub>Al<sub>0.3</sub>As/GaAs [12]. Both samples were covered with a 120 nm Al shadow mask perforated with one micron apertures to enable the measurement of single pairs of dots.
- [25] W. G. van der Wiel, S. De Franceschi, J. M. Elzerman, T. Fujisawa, S. Tarucha, and L. P. Kouwenhoven, *Rev. Mod. Phys.* **75**, 1 (2002).
- [26] M. F. Doty, M. Scheibner, A. S. Bracker, I. V. Ponomarev, T. L. Reinecke, and D. Gammon, *Phys. Rev. B* **78**, 115316 (2008).
- [27] Supplemental material.
- [28] F. Baruffa, P. Stano, and J. Fabian, *Phys. Rev. B* **82**, 045311 (2010).
- [29] M. F. Doty, M. Scheibner, I. V. Ponomarev, E. A. Stinaff, A. S. Bracker, V. L. Korenev, T. L. Reinecke, and D. Gammon, *Phys. Rev. Lett.* **97**, 197202 (2006).
- [30] W. Liu, S. Sanwlani, R. Hazbun, J. Kolodzey, A. S. Bracker, D. Gammon, and M. F. Doty, *Phys. Rev. B* **84**, 121304 (2011).
- [31] For holes, the difference in  $g$ -factor of the InAs QDs and the GaAs tunnel barrier is substantial and  $g_{12} = 0.14$  [37]. For electrons it was found that this difference was negligible with a GaAs barrier, however, it has been found recently that with a GaAs/AlGaAs/GaAs barrier, as used here, this term can also be significant ( $g_{12} = 0.3$ ) [30]. The symmetric Hamiltonian by itself provides a good approximation to the  $2e$  case.
- [32] M. F. Doty, J. I. Climente, A. Greulich, M. Yakes, A. S. Bracker, and D. Gammon, *Phys. Rev. B* **81**, 035308 (2010).
- [33] We have set all  $\gamma_{ii}$  terms to zero at  $B \sim 0$  in Eq. (7).  $\Delta\gamma \gg \Sigma\gamma$  indicates that the local spin-orbit fields  $\beta_1^{so}$ ,  $\beta_2^{so}$  in the two QDs have opposite directions and similar magnitudes. This does not allow for any splitting between the  $T_0$  and the  $T_+/T_-$  states, which must be less than our resolution of  $15 \mu\text{eV}$ .
- [34] D. Kim, S. E. Economou, S. C. Bădescu, M. Scheibner, A. S. Bracker, M. Bashkansky, T. L. Reinecke, and D. Gammon, *Phys. Rev. Lett.* **101**, 236804 (2008).
- [35] J. M. Taylor, J. R. Petta, A. C. Johnson, A. Yacoby, C. M. Marcus, and M. D. Lukin, *Phys. Rev. B* **76**, 035315 (2007).
- [36] M. Ediger, G. Bester, B. D. Gerardot, A. Badolato, P. M. Petroff, K. Karrai, A. Zunger, and R. J. Warburton, *Phys. Rev. Lett.* **98**, 036808 (2007).
- [37] M. F. Doty, J. I. Climente, M. Korkusinski, M. Scheibner, A. S. Bracker, P. Hawrylak, and D. Gammon, *Phys. Rev. Lett.* **102**, 047401 (2009).